ADV MATH SCI JOURNAL
Advances in Mathematics: Scientific Journal **11** (2022), no.8, 671–695
ISSN: 1857-8365 (printed); 1857-8438 (electronic)
https://doi.org/10.37418/amsj.11.8.4

Mathematical modeling and 3D numerical simulation of a solar pond exposed to two solar reflectors

Abdelli Ammar, Bahi Oussama, Ben Boubkeur Soufian, and Kermiche Messaoud

ABSTRACT. The salinity gradient solar pond is simply a pool of water with different mass percentages of salt that collects and stores solar thermal energy.

When solar radiation comes into contact with the water in the basin, it will become the site of two opposing actions, namely the effect of temperature which expands the liquid in its lower parts, thus reducing their density and favoring ascending currents coming from Archimedes' buoyancy and the effect of salinity which increases this density and prevents the liquid from rising. As a result, the converted thermal energy is trapped in the bottom of the basin. The more the temperature of the water increases, the more the fields of application in different uses of this thermal energy widen.

As it is also important to indicate that the high temperature of the storage area allows ponds located in cold areas to save their operating temperatures during the winter period. In an attempt to increase the temperature of the bottom water, we have installed 2 solar reflectors on both sides of the pond which have the role of reflecting solar radiation and returning it to the surface of the pond. This has a positive influence on its thermal performance.

2020 *Mathematics Subject Classification.* 00A71, 76-10.
Key words and phrases. solar pond,solar energy, reflector, discretization, convergence, consistency, stability.
Submitted: 26.07.2022; *Accepted:* 10.08.2022; *Published:* 23.08.2022.

The mathematical model governing the pond dynamics is based on the special 3-direction heat equation with an initial condition and 6 boundary conditions.

The finite volume discretization method in 3D was used, the Camsol software was applied for finer steps.

The numerical results showed that the pond with reflectors recorded a temperature exceeding $13°$C compared to the pond without reflectors.

Convergence, consistency and stability were discussed.

1. Introduction

We live in a world exhausted by fossil fuels, the resulting damage is enormous, we can mainly cite:

- Their combustion produces carbon dioxide which escapes into the atmosphere, thus contributing to increase the greenhouse effect and causing global warming whose terrestrial temperature can be increased by $6°$C by 100 years to come. This can lead to natural disasters such as climate change, rising oceans and their desalination.
- The emanation of CO_2 in nature can also have disastrous consequences on human health such as acute respiratory diseases and cancer.

Solar ponds with salinity gradient can provide a lasting solution to our energy problems but they also pose some problems on the one hand these ponds undergo in winter considerable losses of heat towards the ground and the external walls which negatively influences their performance heat and interfere with their operation.

If we are interested in this work with solar energy, it is because our country has an immense potentiality of sunshine since the nature of the majority of its lands is arid Saharan, which gives us the advantage of being ranked among the sunniest countries in the world. Examples of solar energy harnessing systems include solar panels and natural ponds.

Nevertheless, the latter have the property of converting solar radiation into thermal energy, although most of this energy will be lost in the atmosphere due to convection and/or evaporation.

The salinity gradient solar pond enjoys the advantage of collecting solar radiation and storing it as thermal energy after transformation for a long period of time. Its basic principle is to prevent natural convection from occurring, it consists of 3 areas:

1) Upper convective zone (UCZ): it is generally soft and 30cm thick.
2) Lower convective zone (LCZ): lower thermal energy storage zone, it has a very high salt concentration and is 70 cm thick.
3) Non-convective zone (NCZ): it is located in the middle between the UCZ and the LCZ, consisting of 4 layers with different mass percentages of salt. This prevents the production of any natural convection because of the high density which increases with depth.

This zone is itself made up of several layers of different salinities ranging from 6% to 24% with depth, and we will have the low salinity water floating above the high salinity water.

On the one hand, when the solar radiation reaching the bottom of the basin, it heats the convective layer at the bottom, the density of which must therefore decrease due to thermal expansion.

On the other hand, because of its very high salinity, its density remains high compared to the upper layers, likewise, the salinity gradient which exists in the non-convective layer is favorable to avoid any current. of natural convection.

It is important to emphasize that the installation of solar ponds with salinity gradient in Saharan areas during the winter period suffers the pangs of bad climatic conditions whose temperature can drop enormously and especially during the night, despite the presence of sun during the winter. day, this generates great losses of thermal energy towards the ground and the walls. This negatively affects the proper functioning of the pond and disturbs its physical stability.

In the majority of works dealing with the modeling of salinity gradient solar ponds [2–6], researchers try at all costs to calculate the temperature fields only according to the depth and consider that this variation according to the 2 other horizontal and vertical directions is negligible.

This almost always remains true as long as physical stability is maintained.

Generally, when the sun remains the only energy source which feeds the pond, this one keeps its conservation in salt and consequently there is not an amalgam

at the level of the layers of the NCZ. This is manifested by a thermodynamic equilibrium at the level of the pond.

On another note, it was noted that during the winter season, the heat losses lost by the solar ponds towards the ground and the external walls will be considerable and consequently the solar ponds lose their physical stability and will no longer become functional.

In order to remedy this drawback and permanently increase the temperature of the LCZ storage zone.

We have installed on both sides of the pond 2 identical solar reflectors of the same dimensions ($2m$ long by $1m$ wide) and whose task is to collect solar radiation and send it back to the surface from the pond.

What we bring as a contribution in this present work is the increase of the thermal performance of the solar pond through the commissioning of two solar reflectors.

In this situation, the solar pool will not be powered only by the radiation emitted by the sun, but also by the 2 light sources which are the reflectors. This will automatically lead to a rise in the temperature field.

The hot water extracted from the bottom of the basin will be conveyed towards the outside for various uses, the increase in temperature is proportional with the widening of the fields of application of the ponds.

Our work comes to fill this void and bring a plus to the thermal performance, especially to ponds that are located in cold desert areas. In this work we assume the following hypotheses:

- The pond is energetically supplied by the sun and the 2 reflectors.
- The value of parameters such as the density ρ, the specific capacity C_p and the thermal conductivity k are variable in the NCZ, and depend on the salinity.
- The model of solar radiation adopted in this work is that of Rabl and Nielson [1].
- The effects of weather conditions such as wind and rain are negligible.

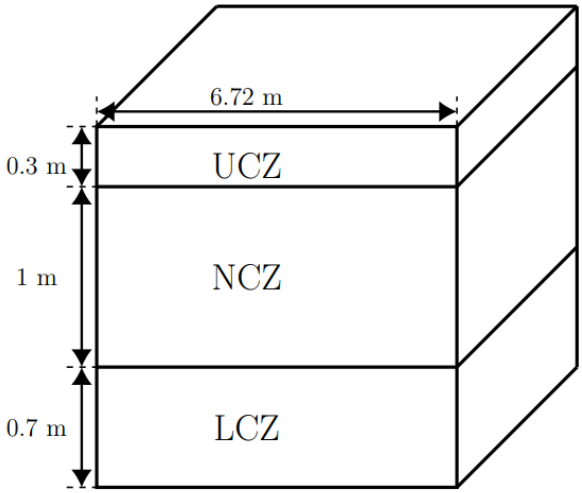

FIGURE 1. Diagram representing the three zones composing the solar pond

2. MATHEMATICAL MODELING OF THE PROBLEM

The mathematical equation that governs the dynamics of the pond is the following:

$$\frac{\partial T}{\partial t} = \frac{k}{\rho C_p}\left(\frac{\partial^2 T}{\partial x^2} + \frac{\partial^2 T}{\partial y^2} + \frac{\partial^2 T}{\partial z^2}\right) - \frac{dE}{\rho C_p dz} + 2S_R, \tag{2.1}$$

where the term $\dfrac{dE}{\rho C_p dz}$ represents the amount of energy reaching the pond water provided by solar radiation and S_R represents the source of energy provided by the solar reflector.

The density ρ, the thermal conductivity k and the specific heat C_p are given by [6]:

$$\rho = 998 - 0.4\,(T - 293.15) + 650s$$
$$k = -2 \times 10^{-5}s^2 - 0.0015s + 0.514$$
$$C_p = 4180 - 4.369\left(\frac{s}{100}\right)\rho + 0.0048\left(\frac{s}{100}\right)^2\rho^2$$

such that s is the salinity.

The model of solar radiation used is a triangle formed by the sun and the 2 reflectors.

a) The sun: is a sphere with a diameter $D = 1.4 \times 10^6 Km$ and a temperature of the order of $5779°k$.

It is located at a distance of $150 \times 10^6 Km$ from the earth. Inside, they take place reactions of nuclear fusion of hydrogen thus releasing energy in the form of radiation which propagates in all the directions and which are actually electromagnetic waves. The emittance of the sun M_0 is given by the following Stefan-Boltzmann law

$$M_0 = \sigma T^4 = 63.24 \times 10^6 W/m^2,$$

where σ is called the Boltzmann constant and is equal to

$$\sigma = 5.67 \times 10^{-8} W/m^2 k^4.$$

The total power emitted by the sun

$$\phi_s = S_s M_0 = \pi D^2 M_0 = 3.85 \times 10^{26} W,$$

where S_s: the surface of the sun $= \pi D^2 = 1.5386 \times 10^{18} m^2$. In this sense, the part of the solar radiation that penetrates will encounter obstacles that weaken or attenuate it, such as absorbers.

b) solar reflectors: they are located on both sides of the pond and have the task of capturing solar radiation and sending it back into the pond. These are 2 giant automated mirrors.

Calculation of average solar power at the equator:

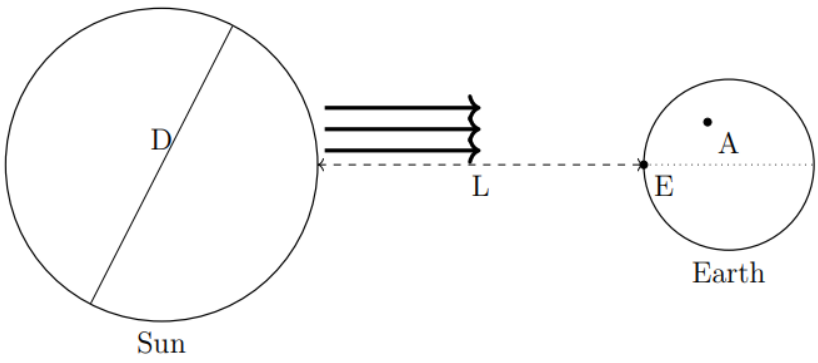

FIGURE 2. The amount of solar energy reaching the equator E and the pond site A

$$P_E = \frac{1}{4}\left(\frac{D}{2L}\right)^2 M_0 = 342W/m^2.$$

E: the equator where the solar radiation is perpendicular.

A: the site of the pond.

α: the angle between the surface normal of point A and the direction of the sun.

L is the distance between the earth and the sun.

This power will be reduced under the effect of the inclination and the atmosphere.

Calculation of the amount of solar radiation received by the pond:

The period of sunshine is fixed from 1/7 to 28/7, the pond is located in a place A with coordinates: Latitude $36°\ 53'\ 59"$ Nord; Longitude $7°\ 46'\ 00"$ Est; and

$$Albedo = \frac{P_{reflexive}}{P_{incident}} = |cos\alpha| \simeq 13\%.$$

So the pond receives an average flux per unit area:

$$342 - \left(\frac{342 \times 13}{100}\right) = 297.54W/m^2.$$

In this work we will consider the 2 reflectors as two light sources that can reflect solar radiation towards the background.

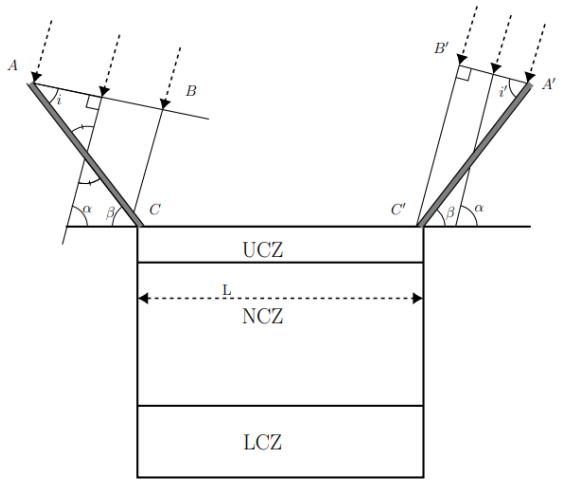

FIGURE 3. Schematic diagram of reflectors

The quantity of energy provided by the 2 reflectors is given by:

$$2Q_{R1} = 2AC\cos\left[(\alpha+\beta)-90\right]\frac{Q_1}{L} = 2AC\sin\left(\alpha+\beta\right)\frac{Q_1}{L}$$

such that AC is the total length of the reflectors.

i: is the angle between the front face of the projected area of the reflectors and the incident light AB.

Q_1: is the amount of solar energy falling on $1m^2$ of surface perpendicular to incident light per unit time.

Q_{R1}, Q_{R2}: the quantities of solar energy reflected by the 1^{st} and 2^{nd} reflectors respectively towards the pond.

The total amount of energy reaching the solar pond (see figure 3) will be the sum of the energy from the sun that directly enters the pond added to the amount of energy that will be reflected from both reflectors which will be considered as two light sources.

$$S = \frac{1}{\rho C_p}\frac{dE}{dz} + 2Q_R = \frac{1}{\rho C_p}\frac{dE}{dz} + \frac{2AC\sin\left(\alpha+\beta\right)Q_1}{L}.$$

In what follows the temperatures of the pond with reflectors will be calculated and measured along the left and right wall represented respectively by the lines A and C and in the center represented by the line B in the direction z as shown in the following figure:

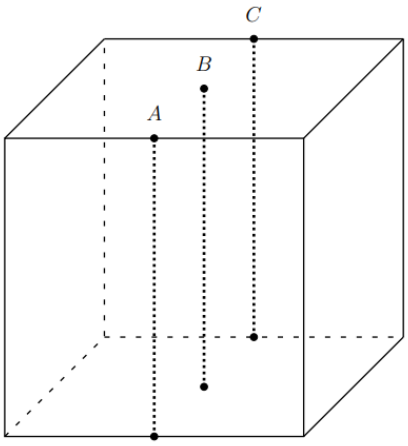

FIGURE 4. Demonstration of the A, B and C lines in the pond

Incorporation of initial and boundary conditions:

The resolution of the equation (2.1) requires the determination of the initial and boundary conditions. In our case, we have only one initial condition and 6 boundary conditions.

Initial condition: Just now $t = 0$, $T(x, y, z, 0) = T_a$.

Boundary conditions:

- $z = z_1$, $T(x, y, z_1, t) = T_a$.
- At the bottom of the pond, the temperature applied to the LCZ zone is given by:

$$z_3 \rho C_p \frac{\partial T}{\partial t} = -k \frac{\partial T}{\partial z} + E_{LCZ} - Q_{out} \tag{2.2}$$

- When $x = 0$ and $y = 0$, the temperature is calculated respectively from the following equations:

$$-k \frac{\partial T}{\partial x}|_{x=0} = C_{ht}(T - T_a) \tag{2.3}$$

$$-k \frac{\partial T}{\partial y}|_{y=0} = C_{ht}(T - T_a) \tag{2.4}$$

- When $x = y = L$ the temperature is calculated respectively from the following equations:

$$-k \frac{\partial T}{\partial x}|_{x=L} = C_{ht}(T - T_a) \tag{2.5}$$

$$-k \frac{\partial T}{\partial y}|_{y=L} = C_{ht}(T - T_a) \tag{2.6}$$

Where C_{ht} is the heat transfer coefficient by free convection on the vertical walls towards the ambient air, this coefficient is estimated at $20W/m^2$.

3. Numerical resolution

Let us apply the finite volume method to discretize the equation governing the transient thermal behavior of the solar pond.

$$\frac{\partial T}{\partial t} = \frac{k}{\rho C_p} \left(\frac{\partial^2 T}{\partial x^2} + \frac{\partial^2 T}{\partial y^2} + \frac{\partial^2 T}{\partial z^2} \right) + S_T, \tag{3.1}$$

such as $S_T = -\dfrac{dE}{\rho C_p dz} + 2S_R$.

Here S_T represents the total energy source and S_R the energy source given by the reflector.

$(x, y, z) \in [0, L_x] \times [0, L_y] \times [0, L_z]$, such as $L_x = L_y = 6,72m$ and $L_z = 2m$.

The computational domain is discretized into $N \times M \times P$ cells with center (x_i, y_j, z_ℓ), (i varying from 0 to $N-1$, j varying from 0 to $M-1$ and ℓ varying from 0 to $P-1$).

It will be assumed that the space steps in each direction $\Delta x = x_{i+\frac{1}{2}} - x_{i-\frac{1}{2}}$, $\Delta y = y_{j+\frac{1}{2}} - y_{j-\frac{1}{2}}$ et $\Delta z = z_{\ell+\frac{1}{2}} - z_{\ell-\frac{1}{2}}$.

The numerical method of finite volumes consists in transforming the continuous problem into a discrete problem possessing a large algebraic system whose matrix dimension depends on the step of discretization, the more the latter tends towards zero, the more the size of the matrix increases, which requires the call for a high-performance computing tool.

The finite volume method is a special version of the weighted residual method where the projection function equals unity.

Particularly in the problems of physical modeling, the smoothness of the step of discretization will be essential since it allows us to approach towards the exact solution.

The finite volume method consists in subdividing the study domain into elementary volumes so that each main node will be contained in each volume which in turn will be delimited by 6 interfaces.

The differential equation will be integrated into each finite elementary volume whose unknown will be represented using an approximation function.

If our choice was based on this method, it is because its implementation is simple and the control volumes are parallelepipeds.

$$\frac{T^{n+1} - T^n}{\Delta t} = \frac{k}{\rho C_p} \int_{z_{\ell-\frac{1}{2}}}^{z_{\ell+\frac{1}{2}}} \int_{y_{j-\frac{1}{2}}}^{y_{j+\frac{1}{2}}} \frac{1}{\Delta x} \left[\left(\frac{\partial T}{\partial x} \right)^n_{x_{i+\frac{1}{2}}} - \left(\frac{\partial T}{\partial x} \right)^n_{x_{i-\frac{1}{2}}} \right] dydz + \frac{k}{\rho C_p} \int_{z_{\ell-\frac{1}{2}}}^{z_{\ell+\frac{1}{2}}} \int_{x_{i-\frac{1}{2}}}^{x_{i+\frac{1}{2}}} \frac{1}{\Delta y} \left[\left(\frac{\partial T}{\partial y} \right)^n_{y_{j+\frac{1}{2}}} - \left(\frac{\partial T}{\partial y} \right)^n_{y_{j-\frac{1}{2}}} \right] dxdz \tag{3.2}$$

$$+\frac{k}{\rho C_p}\int_{y_{j-\frac{1}{2}}}^{y_{j+\frac{1}{2}}}\int_{x_{i-\frac{1}{2}}}^{x_{i+\frac{1}{2}}}\frac{1}{\Delta z}\left[\left(\frac{\partial T}{\partial z}\right)_{z_{\ell+\frac{1}{2}}}^{n}-\left(\frac{\partial T}{\partial z}\right)_{z_{\ell-\frac{1}{2}}}^{n}\right]dxdy$$
$$-\frac{dE}{\rho C_p dz}+2S_R$$

$$\begin{aligned}\frac{T^{n+1}-T^n}{\Delta t}&=\frac{k}{\rho C_p}\left[\frac{T^n_{i+1,j,\ell}-2T^n_{i,j,\ell}+T^n_{i-1,j,\ell}}{(\Delta x)^2}\right]\\&+\frac{k}{\rho C_p}\left[\frac{T^n_{i,j+1,\ell}-2T^n_{i,j,\ell}+T^n_{i,j-1,\ell}}{(\Delta y)^2}\right]\\&+\frac{k}{\rho C_p}\left[\frac{T^n_{i,j,\ell+1}-2T^n_{i,j,\ell}+T^n_{i,j,\ell-1}}{(\Delta z)^2}\right]\\&-\left(\frac{E^n_{\ell+1}-E^n_{\ell-1}}{\rho C_p 2\Delta z}\right)+2\left(\frac{S^n_{R_{\ell+1}}-S^n_{R_{\ell-1}}}{2\Delta z}\right)\end{aligned}\tag{3.3}$$

Let's put $r_x=\dfrac{k\Delta t}{\rho C_p(\Delta x)^2}$; $r_y=\dfrac{k\Delta t}{\rho C_p(\Delta y)^2}$; $r_z=\dfrac{k\Delta t}{\rho C_p(\Delta z)^2}$ et

$$\delta_x^2 T^n=T^n_{i+1,j,\ell}-2T^n_{i,j,\ell}+T^n_{i-1,j,\ell}\tag{3.4}$$

$$\delta_y^2 T^n=T^n_{i,j+1,\ell}-2T^n_{i,j,\ell}+T^n_{i,j-1,\ell}\tag{3.5}$$

$$\delta_z^2 T^n=T^n_{i,j,\ell+1}-2T^n_{i,j,\ell}+T^n_{i,j,\ell-1}\tag{3.6}$$

such as $\delta_x^2,\ \delta_y^2$ and δ_z^2 are the central difference operators in $x,\ y$ and z direction. The equation (3.3) becomes:

$$\begin{aligned}T^{n+1}-T^n&=r_x\delta_x^2T^n+r_y\delta_y^2T^n+r_z\delta_z^2T^n\\&+\Delta t\left[-\left(\frac{E^n_{\ell+1}-E^n_{\ell-1}}{\rho C_p 2\Delta z}\right)+2\left(\frac{S^n_{R_{\ell+1}}-S^n_{R_{\ell-1}}}{2\Delta z}\right)\right].\end{aligned}\tag{3.7}$$

The solution of the equation (3.7) can lead us to a mathematical instability or even a divergence of the solution. To y remedy, we will apply the Peaceman-Rachford approach which consists in dividing the time into 3 fractions, i.e., instead of going from time n to final time $(n+1)$ we will go from $n\longrightarrow n+\dfrac{1}{3}\longrightarrow n+\dfrac{2}{3}\longrightarrow n+1$,

and the equation (3.7) will generate 3 equations:

$$T^{n+\frac{1}{3}} - T^n = r_x\delta_x^2 T^{n+\frac{1}{3}} + r_y\delta_y^2 T^n + r_z\delta_z^2 T^n + \Delta t\left[-\left(\frac{E^n_{\ell+1} - E^n_{\ell-1}}{\rho C_p 2\Delta z}\right) + 2\left(\frac{S^n_{R_{\ell+1}} - S^n_{R_{\ell-1}}}{2\Delta z}\right)\right] \tag{3.8}$$

$$T^{n+\frac{2}{3}} - T^n = r_x\delta_x^2 T^{n+\frac{1}{3}} + r_y\delta_y^2 T^{n+\frac{2}{3}} + r_z\delta_z^2 T^n + \Delta t\left[-\left(\frac{E^n_{\ell+1} - E^n_{\ell-1}}{\rho C_p 2\Delta z}\right) + 2\left(\frac{S^n_{R_{\ell+1}} - S^n_{R_{\ell-1}}}{2\Delta z}\right)\right] \tag{3.9}$$

$$T^{n+1} - T^n = r_x\delta_x^2 T^{n+\frac{1}{3}} + r_y\delta_y^2 T^{n+\frac{2}{3}} + r_z\delta_z^2 T^{n+1} + \Delta t\left[-\left(\frac{E^n_{\ell+1} - E^n_{\ell-1}}{\rho C_p 2\Delta z}\right) + 2\left(\frac{S^n_{R_{\ell+1}} - S^n_{R_{\ell-1}}}{2\Delta z}\right)\right]. \tag{3.10}$$

Each equation generates a tridiagonal system in one space.

In order to calculate the terms of time $T^{n+\frac{1}{3}}, T^{n+\frac{2}{3}}$ et T^{n+1}, let's put

$$S_T = \Delta t\left[-\left(\frac{E^n_{\ell+1} - E^n_{\ell-1}}{\rho C_p 2\Delta z}\right) + \left(\frac{S^n_{R_{\ell+1}} - S^n_{R_{\ell-1}}}{\Delta z}\right)\right],$$

and $r_x = r_y = r_z = \rho$.

$$T^{n+\frac{1}{3}} = \frac{1+\rho\left(\delta_y^2+\delta_z^2\right)}{1-\rho\delta_x^2}T^n + \frac{S_T}{1-\rho\delta_x^2} \tag{3.11}$$

$$T^{n+\frac{2}{3}} = \frac{1+\rho^2\left(\delta_x^2\delta_y^2+\delta_x^2\delta_z^2\right)}{\left(1-\rho\delta_x^2\right)\left(1-\rho\delta_y^2\right)}T^n + \frac{S_T}{\left(1-\rho\delta_x^2\right)\left(1-\rho\delta_y^2\right)} \tag{3.12}$$

$$\begin{aligned} T^{n+1} = {} & \frac{\left(1-\rho\delta_x^2\right)\left(1-\rho\delta_y^2\right)+\rho\delta_y^2\left(1+\rho^2\delta_x^2\delta_y^2+\rho^2\delta_x^2\delta_z^2\right)}{\left(1-\rho\delta_x^2\right)\left(1-\rho\delta_y^2\right)\left(1-\rho\delta_z^2\right)}T^n \\ & + \frac{\rho\delta_x^2\left(1-\rho\delta_x^2\right)\left(1-\rho\delta_y^2\right)\left(1+\rho\delta_y^2+\rho\delta_z^2\right)}{\left(1-\rho\delta_x^2\right)\left(1-\rho\delta_y^2\right)\left(1-\rho\delta_z^2\right)}T^n \\ & + \frac{S_T}{1-\rho\delta_x^2}\left[1+\frac{\rho\delta_y^2}{1-\rho\delta_y^2}\right]. \end{aligned} \tag{3.13}$$

Eventually we get a system of algebraic equations of the form $Y = AX+B$, comprising 64 equations with 96 unknowns. The initial condition and the boundary conditions make it possible to eliminate 32 unknowns.

As for the numerical resolution of this system of equations, we use the iterative method of Gauss-Seïdel because of its great stability with respect to rounding errors.

Calculation of solar radiation reaching the solar pond:

The solar radiation model applied is that of Rabl-Nilson

$$E = E_s e^{-\mu z}.$$

Here, E_s represents the solar radiation reaching the surface and μ is equal to $0.5m^{-1}$ and is called the extinction coefficient.

We consider that the water is moderately turbid and that the sky is clear (absence of clouds) during the period of sunshine.

Solar radiation calculations will be done every 3 hours, daybreak is assumed at 5 am and noon will be the time when the sun will be perpendicular to the pond.

TABLE 1. Calculation moments of solar radiation

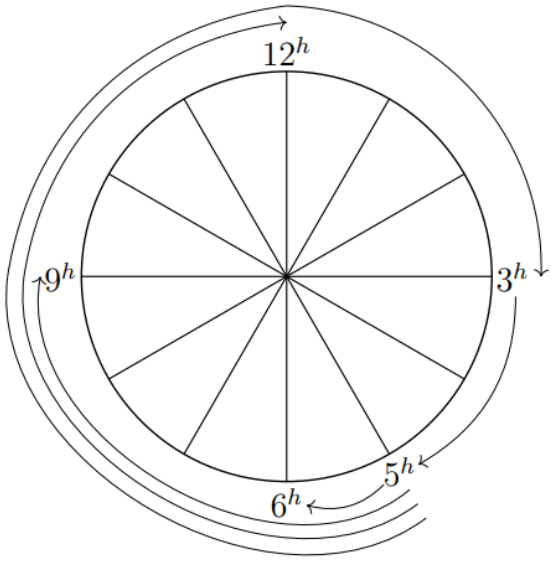

Schedule (hour) (n_i)	0^h	3^h	6^h	9^h	12^h	15^h	18^h	21^h
Solar energy E_i (W/m^2)	0	0	94.27	183.1	297.54	240.32	97.66	0

Average daily energy

$$E_m = \frac{\sum E_i}{N_i} = \frac{912.89}{8} = 114.11 W/m^2.$$

The table 3 gives the energy values in the different levels of the pond:

TABLE 2. The amount of energy in the different depth levels

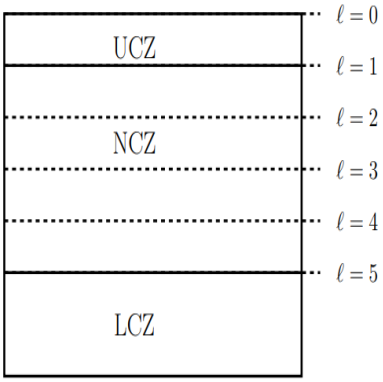

depth index (ℓ)	Depth (z) (metre)	Average solar energy (W/m^2)	Average energy provided by reflectors (W/m^2)	Total energy (W/m^2)
$\ell = 0$	0	114.11	43.56	157.67
$\ell = 1$	0.3	98.22	37.46	135.68
$\ell = 2$	0.55	86.71	33.1	119.81
$\ell = 3$	0.8	76.58	29.18	105.76
$\ell = 4$	1.05	67.32	25.7	93.02
$\ell = 5$	1.3	59.33	22.65	81.98

Concerning the other meshes such as normal, fine and finer, we used the Camsol software which is designed for the numerical resolution of these large algebraic systems.

The latter uses several multigrid levels where each level corresponds to a mesh and a choice of function.

Thus, with each transition from one mesh to another finer, the number of degrees of freedom decreases and the meshes constructed thus obtained will be automatic.

The alignment of these meshes can be carried out thanks to an option using the successive refinements of the aligned meshes.

4. RESULTS AND DISCUSSIONS

4.1. **Choice of meshes.** This work consists in calculating the temperature as a function of time through the following 4 meshes:

- 1^{st} mesh: discretization steps $h = \frac{1}{4}$, system of equations comprising 64 equations with 96 unknowns.

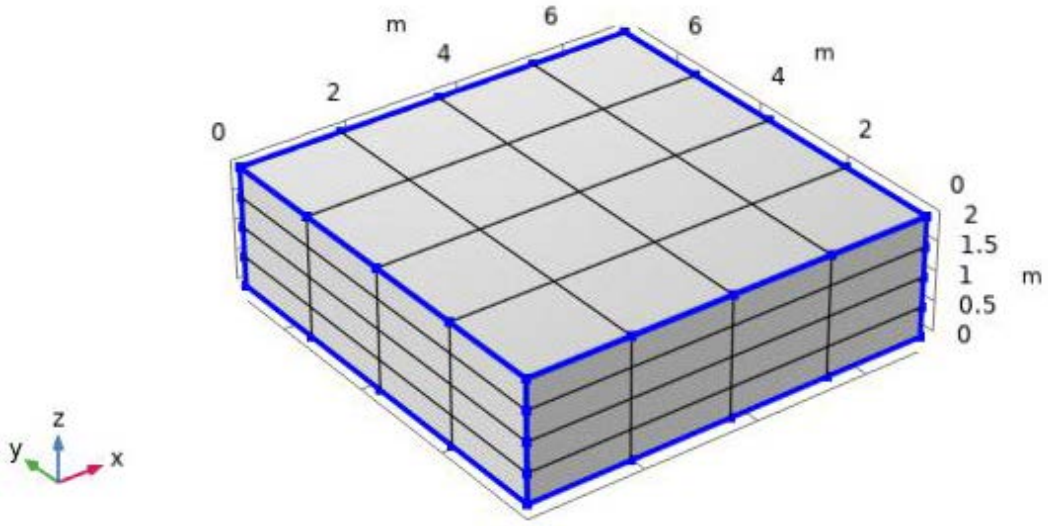

FIGURE 5. The discretization steps $h = \frac{1}{4}$

- 2^{nd} mesh: normal mesh, mesh consists of 4238 domain elements, 840 boundary elements, and 92 edge elements.

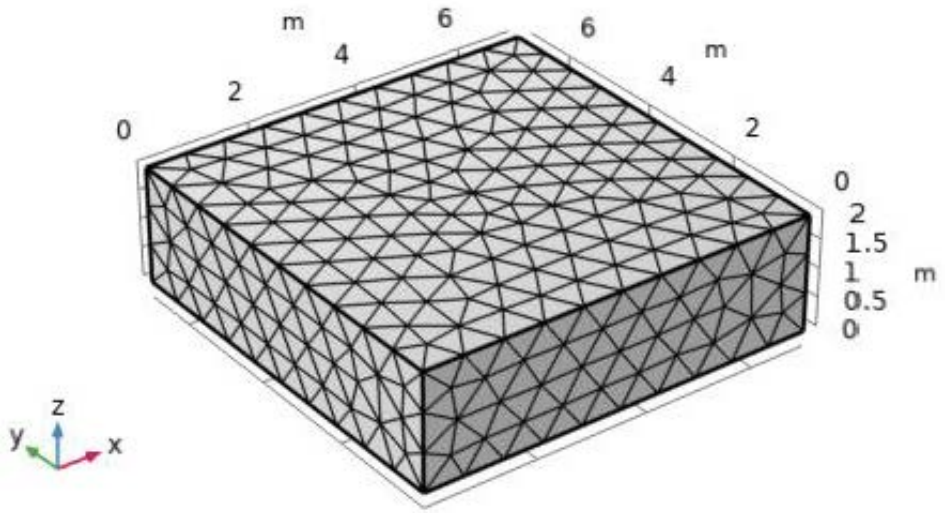

FIGURE 6. Mesh normal

- 3^{rd} mesh: fine mesh, mesh consists of 8673 domain elements, 1252 boundary elements, and 120 edge elements.

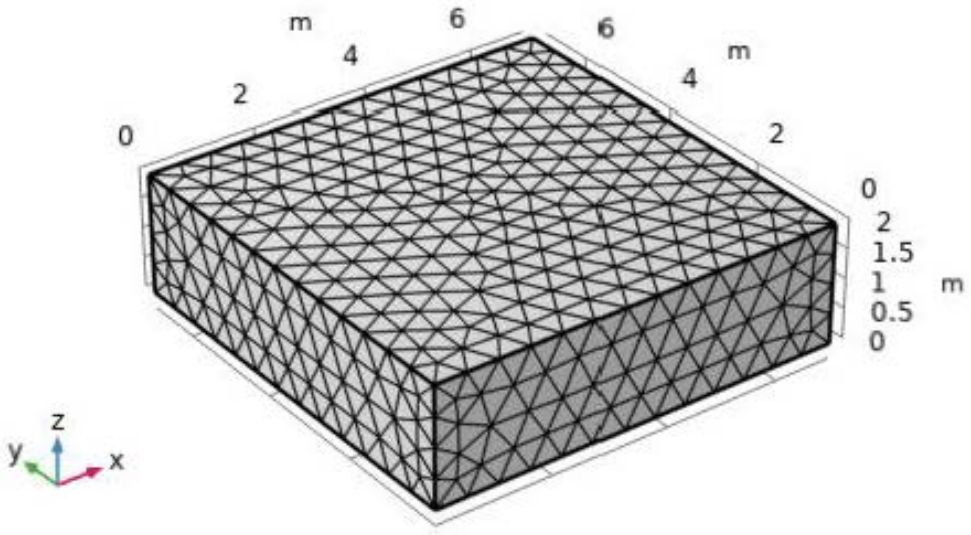

FIGURE 7. Fine mesh

- 4^{th} mesh: finer mesh, mesh consists of 27861 domain elements, 2460 boundary elements, and 164 edge elements.

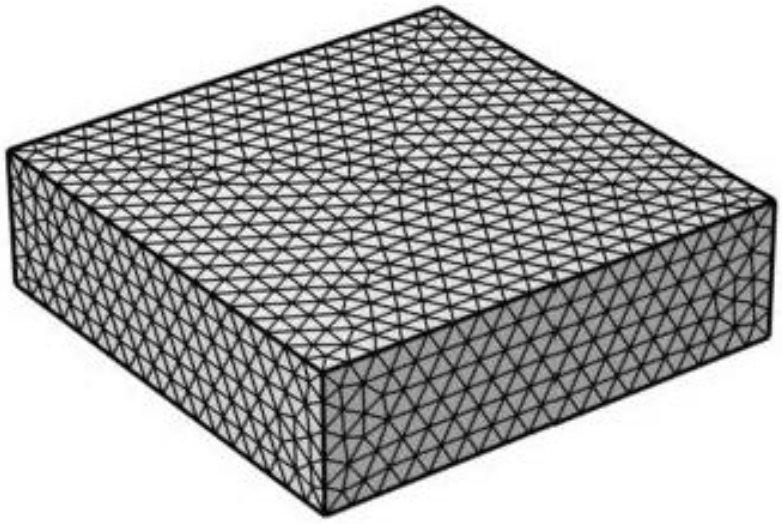

FIGURE 8. Finer mesh

4.2. **The temperature profile.** The temperature profile according to the salinity is given with respect to points A, B and C which are located respectively to the left, in the middle and to the right of the NCZ zone.

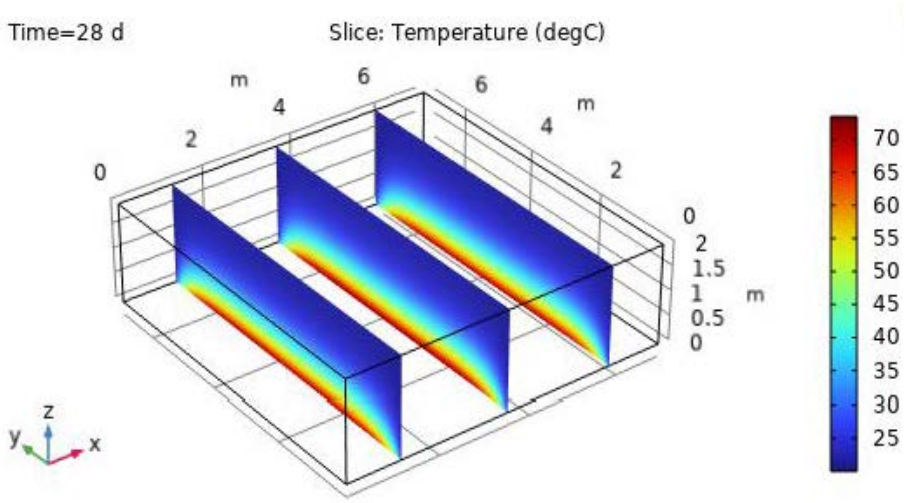

FIGURE 9. Temperature profile at points A, B and C as a function of salinity for a pond without reflectors

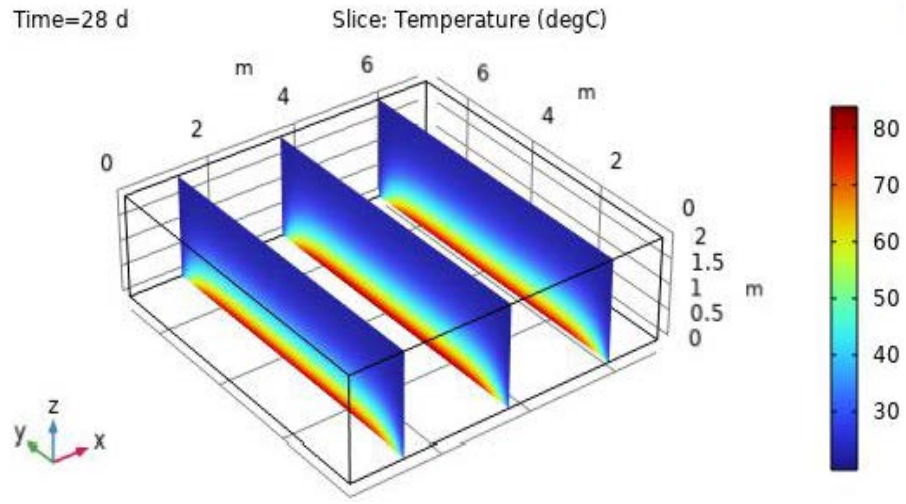

FIGURE 10. Temperature profile at points A, B and C as a function of salinity for a pond with reflectors

TABLE 3. The evolution of temperature as a function of salinity for a pond without reflectors

Coordinates				Reference solution	Numerical solution		
Position	$X(m)$	$Y(m)$	$Z(m)$	Finer	$h = \frac{1}{4}$	normal	Fine
Point A	1.68	3.36	0.55	36.23	35.61	35.67	35.98
	1.68	3.36	0.8	48.43	47.55	48.01	48.28
	1.68	3.36	1.05	59.54	58.76	59.07	59.36
	1.68	3.36	1.3	71.08	70.21	70.52	70.89
Point B	3.36	3.36	0.55	37.29	36.51	36.78	37.06
	3.36	3.36	0.8	49.71	49.08	49.19	49.49
	3.36	3.36	1.05	60.65	60.25	60.36	60.61
	3.36	3.36	1.3	72.34	71.88	72.1	72.26
Point C	5.04	3.36	0.55	36.09	35.5	35.89	36
	5.04	3.36	0.8	48.22	47.66	47.68	47.98
	5.04	3.36	1.05	59.56	59.07	59.11	50.43
	5.04	3.36	1.3	71.13	70.29	70.52	70.99

TABLE 4. The evolution of temperature as a function of salinity for a pond with reflectors

Coordinates				Reference solution	Numerical solution		
Position	$X(m)$	$Y(m)$	$Z(m)$	Finer	$h = \frac{1}{4}$	normal	Fine
Point A	1.68	3.36	0.55	40.28	39.82	39.92	40.07
	1.68	3.36	0.8	55.57	55.26	55.38	55.41
	1.68	3.36	1.05	70.31	69.65	69.85	70.08
	1.68	3.36	1.3	84.29	83.92	84.01	84.19
Point B	3.36	3.36	0.55	41.07	40.48	40.61	40.86
	3.36	3.36	0.8	56.18	55.72	56	56.12
	3.36	3.36	1.05	71.87	71.28	71.42	71.7
	3.36	3.36	1.3	85.22	84.78	84.99	85.16
Point C	5.04	3.36	0.55	40.12	39.38	39.6	39.79
	5.04	3.36	0.8	55.27	55	55.13	55.28
	5.04	3.36	1.05	70.64	70.12	70.29	70.34
	5.04	3.36	1.3	84.38	84.01	84.09	84.12

Discussion:

The concept of convergence of a diagram expresses its property to tend towards the exact solution of the problem treated for mesh parameters, such as the number of nodes tending towards infinity.

It is possible to show that convergence is assured if the numerical scheme adopted in this work is both stable and consistent.

The stability of a diagram translates its faculty to adopt a regular behavior during the introduction of any disturbance due for example to the bad calculation of a boundary condition or an initial condition.

A scheme is said to be stable if any disturbance of digital origin is damped or at best not amplified. It will be said to be unstable if, on the contrary, any disturbance, however minimal it may be, is amplified over time or in space.

If we used in this work the method of Douglas-Rachford to discretize the fundamental equation which governs the dynamics of the movement it is to ensure an unconditional mathematical stability.

This method is also called the method of fractional steps which consists of dividing time into 3 fractions of $n \longrightarrow n+\frac{1}{3} \longrightarrow n+\frac{2}{3} \longrightarrow n+1$.

To determine the truncation error and the stability factor, let's apply the Douglas-Rachford approach.

Let $r_x = r_y = r_z = \rho$ and assume that the source of energy that powers the solar pond is zero. Let's eliminate the indices (i, j, ℓ).

The system of equations (3.8), (3.9) and (3.10) can be written:

$$T^{n+\frac{1}{3}} - T^n = \frac{\Delta t}{k^2}\left(\delta_x^2 T^{n+\frac{1}{3}} + \delta_y^2 T^n + \delta_z^2 T^n\right) \tag{4.1}$$

$$T^{n+\frac{2}{3}} - T^{n+\frac{1}{3}} = \frac{\Delta t}{k^2}\delta_y^2\left(T^{n+\frac{2}{3}} - T^n\right) \tag{4.2}$$

$$T^{n+1} - T^{n+\frac{2}{3}} = \frac{\Delta t}{k^2}\delta_z^2\left(T^{n+1} - T^n\right) \tag{4.3}$$

in more general split form, we can write:

$$\left(1-\rho\delta_x^2\right)T^{n+(*)} = \left[1+\rho\left(\delta_y^2+\delta_z^2\right)\right]T^n \tag{4.4}$$

$$\left(1-\rho\delta_y^2\right)T^{n+(**)} = T^{n+(*)} - \rho\delta_y^2 T^n \tag{4.5}$$

$$\left(1-\rho\delta_z^2\right)T^{n+1} = T^{n+(**)} - \rho\delta_z^2 T^n \tag{4.6}$$

Let's eliminate $T^{n+(*)}$ et $T^{n+(**)}$, we obtain:

$$\begin{aligned}\left(1-\rho\delta_x^2\right)\left(1-\rho\delta_y^2\right)\left(1-\rho\delta_z^2\right)T^{n+1} &= \rho^2\left(\delta_x^2\delta_y^2+\delta_y^2\delta_z^2+\delta_x^2\delta_z^2\right)T^n \\ &\quad + \left(1-\rho^3\delta_x^2\delta_y^2\delta_z^2\right)T^n\end{aligned} \tag{4.7}$$

Both the coefficients in (4.7) are consistent 27 point operators. The equation (4.7) can still be written:

$$T^{n+1} = T^n + \rho\left(\delta_x^2+\delta_y^2+\delta_z^2\right)T^{n+1} - \rho^2\left(\delta_x^2\delta_y^2+\delta_y^2\delta_z^2+\delta_x^2\delta_z^2\right)\left(T^{n+1}-T^n\right) + \rho^3\delta_x^2\delta_y^2\delta_z^2\left(T^{n+1}-T^n\right) \tag{4.8}$$

Using the Taylor series expansions and the relations

$$T_x = \nabla^2 T,\ T_{xx} = \nabla^4 T \text{ où } \nabla^2 T = \frac{\partial^2 T}{\partial x^2}+\frac{\partial^2 T}{\partial y^2}+\frac{\partial^2 T}{\partial z^2}$$

The local truncation error of the Douglas-Rachford shema is

$$-\frac{1}{12}\rho k^4\left(\frac{\partial^4 T}{\partial x^4}+\frac{\partial^4 T}{\partial y^4}+\frac{\partial^4 T}{\partial z^4}\right)-\frac{\rho^2 k^4}{2}\nabla^4 T$$

let's put

$$T^{n+(*)} = T^{n+(**)} = G^{n+1} \tag{4.9}$$

We can write:

$$T^{n+(*)} = G^n + \left(1-\rho\delta_y^2\right)\left(1-\rho\delta_z^2\right)\left(G^{n+1}-G^n\right) \tag{4.10}$$

$$T^{n+(**)} = G^n + \left(1-\rho\delta_z^2\right)\left(G^{n+1}-G^n\right) \tag{4.11}$$

A standart stability analysis shows that the overall amplification factor is

$$\lambda = \frac{1+A_1A_2+A_1A_3+A_2A_3+A_1A_2A_3}{(1+A_1)(1+A_2)(1+A_3)}$$

where, as before,

$$A_i = 4\rho\sin^2\left(\frac{\beta_i k}{2}\right), i = 1,2,3.$$

As it is also interesting to note that

$$r_x + r_y + r_z = 0.4295 \leq \frac{1}{2}.$$

This further shows that the numerical scheme used is stable.

Error calculation:

In this work, the mesh finer solution was taken as the reference solution. The relative error in percentage is defined by:

$$\left|\frac{Reference\ solution - Considered\ solution}{Reference\ solution}\right| \times 100.$$

The relative errors of the simulation results are given in the following two tables:

TABLE 5. Relative errors for a solar pond without reflectors

Position	$X(m)$	$Y(m)$	$Z(m)$	Reference solution	Relative error %		
					$h = \frac{1}{4}$	normal	fine
Point A	1.68	3.36	0.55	36.23	1.71	1.54	0.69
	1.68	3.36	0.8	48.43	1.82	0.86	0.31
	1.68	3.36	1.05	59.54	1.31	0.79	0.3
	1.68	3.36	1.3	71.08	1.22	0.78	0.27
Point B	3.36	3.36	0.55	37.29	2.09	1.37	0.62
	3.36	3.36	0.8	49.71	1.27	1.05	0.44
	3.36	3.36	1.05	60.65	0.66	0.48	0.06
	3.36	3.36	1.3	72.34	0.63	0.33	0.11
Point C	5.04	3.36	0.55	36.09	1.63	0.55	0.25
	5.04	3.36	0.8	48.22	1.16	1.2	0.5
	5.04	3.36	1.05	59.56	0.82	0.75	0.22
	5.04	3.36	1.3	71.13	1.18	0.86	0.2

TABLE 6. Relative errors for a solar pond with reflectors

Position	$X(m)$	$Y(m)$	$Z(m)$	Reference solution	Relative error %		
					$h = \frac{1}{4}$	normal	fine
Point A	1.68	3.36	0.55	40.28	1.14	0.89	0.52
	1.68	3.36	0.8	55.57	0.55	0.34	0.28
	1.68	3.36	1.05	70.31	0.93	0.65	0.32
	1.68	3.36	1.3	84.29	0.43	0.33	0.11
Point B	3.36	3.36	0.55	41.07	1.43	1.12	0.51
	3.36	3.36	0.8	56.18	0.81	0.32	0.1
	3.36	3.36	1.05	71.87	0.82	0.62	0.23
	3.36	3.36	1.3	85.22	0.51	0.26	0.07
Point C	5.04	3.36	0.55	40.12	1.84	1.29	0.82
	5.04	3.36	0.8	55.27	0.48	0.25	0.01
	5.04	3.36	1.05	70.64	0.73	0.49	0.42
	5.04	3.36	1.3	84.38	0.43	0.34	0.3

The tables (5) and (6) given, above, show that this error decreases as the step of discretization tends towards zero, ie, that the number of nodes tends to infinity. This shows a tendency of convergence of the approximate solution towards the exact solution, thus corroborating the theoretical convergence result given by proposition (11.6) of the reference [14]. We therefore deduce that the numerical

scheme adopted is consistent. By referring to the Lax-Milligram theorem which states that any stable and consistent numerical scheme implies that it is convergent. So the scheme adopted in our work is convergent.

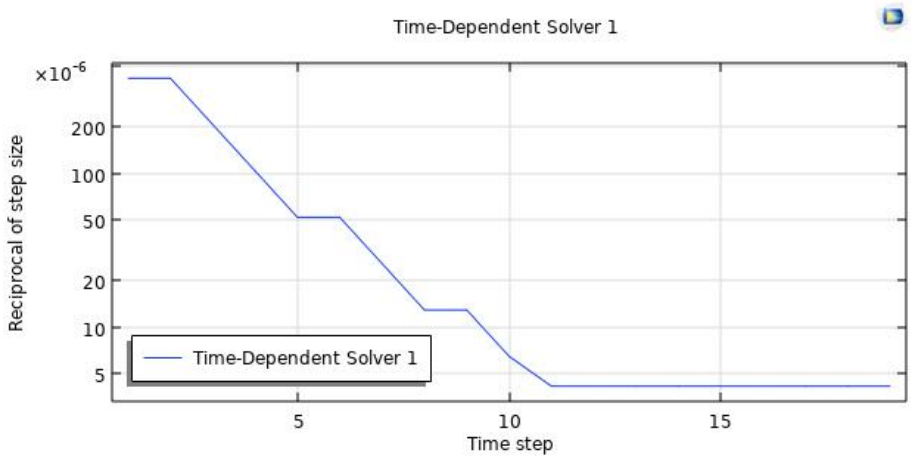

FIGURE 11. Profile convergence diagram of the temperature of the reference solution

On another register, we noted the following points:

- the pond fed by the sun and the 2 reflectors registers a temperature exceeding almost $13°$C compared to the pond without reflectors.
- the growth in temperature is very accelerated during the first 3 weeks to begin to stabilize in the 4^{th} week.
- more intense heating in the central part of the pool represented by point B, than at the periphery represented by points A and C due to heat loss at wall level.
- for a given layer the temperature range can go up to $1°$C because of the permanent presence of solar radiation hitting the center of the basin.
- the layers of the NCZ zone have retained their mass concentrations, this shows that the pond is physically stable and the thermodynamic equilibrium of the LCZ storage zone is maintained.
- the installation of reflectors in sunny Saharan areas is essential because they contribute to raising the temperature of the pond.

5. Conclusion

- As part of this work, we considered a heat transfer inside a solar pond equipped with two reflectors.
- This work came to fill a void which consists in increasing the temperature at the bottom of the pond (LCZ) during the winter season.
- This transfer is governed by the heat equation in 3 spatial dimensions with appropriate initial and boundary conditions.
- The finite volume method together with the Gauss-Seidel scheme was used to discretize the governing equation which is of the parabolic type.
- The numerical results showed that there is an increase in heat of the order of 62% if the pond has two reflectors compared to the pond without reflectors.
- The decrease in the relative error is proportional to the fineness of the spatial and temporal discretization step.
- We hope that similar work will be carried out to see firsthand if the pond retains its physical stability, in other words there will be no more amalgamation of the different layers of the NCZ.

Nomenclature

C_p : Specific heat $[kJ/kg^{\circ}C]$;
E : Radiation intensity $[w/m^2]$;
h : Heat Transfer Coefficient $[w/m^{2\circ}C]$;
k : Heat Conductivity Coefficient $[w/m^{\circ}C]$;
q or Q: Heat transfer rate $[w/m^2]$;
s : Salinity of the brine $[\%]$;
T : Temperature $[^{\circ}C]$;
t : Time [sec];
μ : Extinction Coefficient of Transmission Function $[m-1]$;
ρ : Density $[kg/m^3]$.

References

[1] A. Rabl, C.E. Nielsen: *Solar ponds for space heating*, Solar Energy, **17**(1) (1975), 1-12.

[2] S. TUNDEE, P. TERDTOON, P. SAKULCHANGSATJATAI, R. SINGH, A. AKBARZADEH: *Heat extraction from salinity-gradient solar ponds using heat pipe heat exchangers*, Elsevier, Solar Energy, (2010),1706-1716.

[3] K.R. AGHA: *The thermal characteristics and economic analysis of a solar pond coupled low temperature multi stage desalination plant*, Elsevier, Solar Energy, **83** (2009), 501-510.

[4] J.R. HULL, D.L. BUSHNELL, D.G. SEMPSROTE, A. PENA: *Comparative performance evaluation of fertiliser solar pond under simulated conditions*, Elsevier, Renewable energy, **28**(3) (2003), 455-466.

[5] A.K. SAXENA, S. SUGANDHI, M. HUSAIN: *Significant depth of ground water table for thermal performance of salt gradient solar pond*, Elsevier, Renewable Energy, **34**(3) (2009), 790-793.

[6] M.R. JAEFARZADEH: *Thermal behavior of a small salinity-gradient solar pond with wall shading effect*, Elsevier, Solar energy, **77** (2004), 281-290.

[7] R.B. MANSOUR, C.T. NGUYEN, N. GALANIS: *Numerical study of transient heat and mass transfer and stability in a salt-gradient solar pond*, Elsevier,International Journal of Thermal Sciences, **43**(8) (2004), 779-6790.

[8] MAZIDI, MOHSEN AND SHOJAEEFARD, MOHAMMAD HASSAN AND MAZIDI, MOHAMMAD SH AND SHOJAEEFARD, HOSSEIN: *Two-dimensional modeling of a salt-gradient solar pond with wall shading effect and thermo-physical properties dependent on temperature and concentration*, Springer, Journal of Thermal Science, (2011), 362-370.

[9] R. BOUDHIAF, A.B. MOUSSA, M. BACCAR: *A two-dimensional numerical study of hydrodynamic, heat and mass transfer and stability in a salt gradient solar pond*, Molecular Diversity Preservation International, Energies, **5**(10) (2012), 3986-4007.

[10] R. DARROS-BARBOSA, M.O. BALABAN, A.A. TEIXEIRA: *Transient performance of a two-dimensional salt gradient solar pond—A numerical study*, Wiley Online Library, International journal of energy research, **20**(8) (1996), 713-731.

[11] B.R. MATTHEIJ, H. SISSAOUI, A. ABDELLI, M. KERMICHE, G. BARKER-READ: *Comparison of three solar ponds with different salts through bi-dimensional modeling*, Solar Energy **116** (2015), 56-68.

[12] M. GIESTAS, H. PINA, A. JOYCE: *The influence of radiation absorption on solar pond stability*, Elsevier, International journal of heat and mass transfer, **39**(18) (1996), 3873-3885.

[13] R.H. PERRY, D.W. GREEN, J.O. MALONEY: *Perry's Chemical Engineers' Handbook (ed.)*, McGraw-Hill, Seventh, International edition, 1997.

[14] R.M.M. MATTHEIJ, S.W. RIENSTRA, J.H.M. BOONKKAMP, T. THIJE: *Partial differential equations: modeling, analysis, computation*, SIAM press , 2005.

[15] B.M. MATTHEIJ, H. SISSAOUI, A. ABDELLI, M. KERMICHE, G. BARKER-READ: *The effect of thermodiffusion on the stability of a salinity gradient solar pond*, Elsevier, International journal of heat and mass transfer **48** (2015), 4633-4639.

[16] L. MATTHEIJ, D. PETER, R.D. RICHTMYER: *Survey of the stability of linear finite difference equations*, Wiley Online Library, Communications on pure and applied mathematics **9** (1956), 267-293.

[17] J.F. SCHEID: *méthodes numériques pour la dynamique des fluides*,Institut E. Cartan UMR, Institut E. Cartan UMR (2007), 2011-2012.

[18] R. BEN MANSOUR: *Étude numérique du comportement transitoire d'un étang solaire à gradient de salinité*, National Library of Canada, Ottawa (2005), 267-293.

DEPARTMENT OF MATHEMATIC
UNIVERSITY OF TAMANRASSET
ANNABA,
ALGERIA.
Email address: abdelli_ammar@yahoo.fr

DEPARTMENT OF PREPARATORY CLASS
NATIONAL POLYTECHNIC INSTITUTE OF CONSTANTINE
ALI MENDJELI, CONSTANTINE,
ALGERIA.
Email address: bahi.oussama2@gmail.com

UNIVERSITÉ OF TAMANRASSET, BP 1327, TAMANRASSET 11000, ALGERIA.
TAMANRASSET,
ALGERIA.
Email address: soufishou@gmail.com

LABORATOIRE DE RECHERCHE LANOS
UNIVERSITÉ BADJI MOKHTAR, BP 12, ANNABA 23000, ALGERIA.
ANNABA,
ALGERIA.
Email address: kermiche_mgp@yahoo.fr